BCS theory for $s+g$-wave superconductivity in borocarbides $Y(Lu)Ni_2B_2C$

Qingshan Yuan[1,2] and Peter Thalmeier[1]
[1]*Max-Planck-Institut für Chemische Physik fester Stoffe, Nöthnitzer Strasse 40, 01187 Dresden, Germany*
[2]*Pohl Institute of Solid State Physics, Tongji University, Shanghai 200092, People's Republic of China*
(Received 16 January 2003; revised manuscript received 21 August 2003; published 3 November 2003)

The $s+g$ mixed gap function $\Delta_{\mathbf{k}}=\Delta[(1-x)-x\sin^4\theta\cos 4\phi]$ (x: weight of the g-wave component) has been studied within BCS theory. By suitable consideration of the pairing interaction, we have confirmed that the coexistence of s and g waves, as well as the state with equal s and g amplitudes (i.e., $x=1/2$) may be stable. This provides the semiphenomenological theory for the $s+g$-wave superconductivity with point nodes which has been observed experimentally in borocarbide YNi_2B_2C and possibly in $LuNi_2B_2C$.

DOI: 10.1103/PhysRevB.68.174501 PACS number(s): 74.20.Rp, 74.20.Fg, 74.70.Dd

I. INTRODUCTION

The rare-earth nickel borocarbides RNi_2B_2C ($R=$Y, Lu, Tm, Er, Ho, and Dy) have attracted great interest in recent years due to superconductivity (SC) as well as its possible coexistence with antiferromagnetic order.[1,2] It has initially been thought that these materials can be understood by a largely isotropic s-wave pairing via the conventional electron-phonon coupling.[3] However, various recent experimental results particularly on the two nonmagnetic borocarbides $Y(Lu)Ni_2B_2C$, including specific heat,[4–7] thermal conductivity,[8,9] Raman scattering,[10] NMR relaxation rate,[11] photoemission spectroscopy,[12] scanning tunneling microscopy, and spectroscopy,[13] have unambiguously shown that the gap function is highly anisotropic (with anisotropy ratio[8] $\Delta_{\min}/\Delta_{\max}\leqslant 10^{-2}$ in YNi_2B_2C). For example, the $\sqrt{H}$ dependence of the specific heat in the vortex state indicates a superconducting state with nodal excitations.[4–6] The T^3 power law behavior of the spin-lattice relaxation rate[11] also suggests the existence of nodes. Very recently, compelling evidence has been presented by Izawa *et al.* from the angular-dependent thermal conductivity in a magnetic field that the gap function of YNi_2B_2C has point nodes which are located along the [1,0,0] and [0,1,0] directions.[8] The same conclusion can be also drawn from the angular-dependent specific heat data.[7] A highly anisotropic s-wave gap (with possible nodes) was also discovered in $LuNi_2B_2C$ by thermal conductivity measurements as a function of temperature and field strength.[9] Thus the previous isotropic s-wave theory has to be critically reconsidered.

Recently Maki *et al.* have proposed that the so called $s+g$-wave spin singlet gap function for $Y(Lu)Ni_2B_2C$ superconductors, i.e.,[14,15,8]

$$\Delta_{\mathbf{k}}=\frac{\Delta}{2}(1-\sin^4\theta\cos 4\phi), \tag{1}$$

is consistent with the experimental observation. Here θ,ϕ are the polar and azimuthal angles of $\mathbf{k}$, respectively. The second "g-wave" contribution is given by a fourth degree fully symmetric (A_{1g}) basis function $\psi^{(4)}(\theta,\phi)$ in tetragonal D_{4h} symmetry which is, up to a constant, equal to the real "tesseral harmonic" function $Z^c_{44}(\theta,\phi)=(1/\sqrt{2})[Y^4_4(\theta,\phi)+Y^{-4}_4(\theta,\phi)]$. We have

$$\psi^{(4)}(\theta,\phi)=k_x^4+k_y^4-6k_x^2k_y^2=\sin^4\theta\cos 4\phi. \tag{2}$$

In the gap function (1), the amplitudes of s and g components are assumed to be equal. Thus 4 (and only 4) point nodes at $\theta=\pi/2$ and $\phi=0,\pi/2,\pi,3\pi/2$ are realized, see the middle panel of Fig. 1. This is exactly what has been observed experimentally.[8] Based on the above gap function quite a few physical properties have been calculated such as thermal conductivity,[8] Raman spectra,[16] sound attenuation,[17] etc., and good agreement with the experimental results is obtained.

On the other hand, there is no symmetry reason for the constraint of equal amplitudes of s and g. More generally, the $s+g$ gap function can be described by

$$\Delta_{\mathbf{k}}=\Delta[(1-x)-x\sin^4\theta\cos 4\phi]=\Delta f(\theta,\phi) \tag{3}$$

with a tuning parameter x characterizing the weight of the g-wave component. Obviously Eq. (1) corresponds to the special case $x=1/2$. If $x<1/2$, the s wave is dominant and the nodes will be removed; while if $x>1/2$, the g wave has a strong weight and will contribute eight line nodes. The three different cases have been shown in the xy plane in Fig. 1.

The natural question then arises of how to understand the origin of the above $s+g$ hybrid pairing. So far, a microscopic theory for the pairing potential is not available which might be complicated due to the complex Fermi surface of borocarbides[18] and the possibility of strongly anisotropic Coulomb interactions. As a first step, however, it is necessary to investigate phenomenologically how the $s+g$ state can be realized by constructing an appropriate pairing potential. This is the topic of the present work. As shown below, within BCS weak-coupling theory we have found that a stable coexistence of s and g waves requires a pairing potential which includes the cross term between s- and g-wave functions. In particular, we will show how the fine-tuning $x=1/2$ $s+g$ can be realized almost independent of temperature below T_c.

A similar issue has been addressed by Lee and Choi[19] in their theory to explain Raman scattering data, but no complete study was presented. First, they do not consider the θ dependence of the g-wave part, i.e., implicitly assume a gap function with cylindrical symmetry. Second, they adopt gap models with a strong g component. As shown before in Fig. 1, they will exhibit eight line nodes, which are inconsistent with the experimental results[8] which have revealed four point nodes.

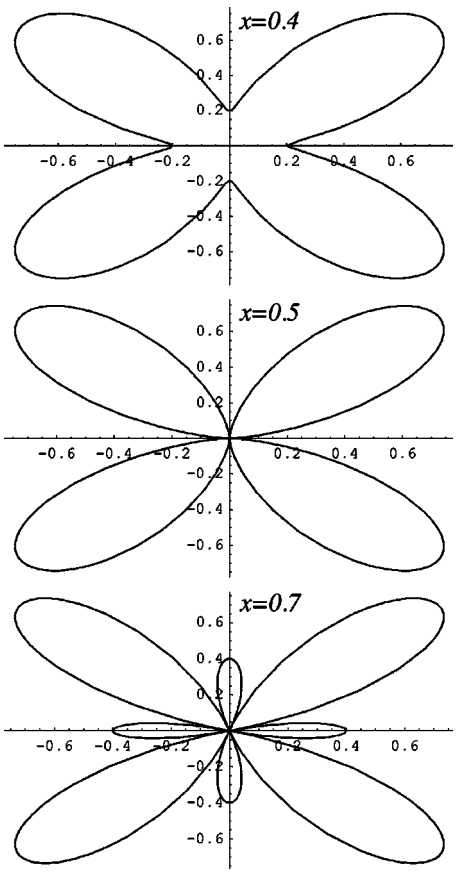

FIG. 1. The xy-plane ($\theta=\pi/2$) polar plots of the $s+g$ wave gap $|\Delta_{\mathbf{k}}|$ for various tuning parameters x.

II. PAIRING INTERACTION AND BCS THEORY FOR THE $s+g$ WAVE STATE

In view of the orthogonality of s- and g-wave functions in Eq. (3), one may naturally express the pairing potential as sum of two separable parts whose weight is given by two parameters V_s and V_g:[20]

$$V_{\mathbf{kk}'}=-[V_s+V_g\psi^{(4)}(\theta,\phi)\psi^{(4)}(\theta',\phi')]. \tag{4}$$

Here the unprimed and primed angles correspond to $\mathbf{k}$ and $\mathbf{k}'$, respectively. Each term in Eq. (4) is separable with respect to wave vectors $\mathbf{k}$ and $\mathbf{k}'$.

Here we try to propose a pairing potential, similar to that used in Ref. 19 for the cylindrical gap, by adding another mixing term V_{sg}:

$$V_{\mathbf{kk}'}=-\{V_s+V_g\psi^{(4)}(\theta,\phi)\psi^{(4)}(\theta',\phi')+V_{sg}[\psi^{(4)}(\theta,\phi)+\psi^{(4)}(\theta',\phi')]\}. \tag{5}$$

Before we proceed to solve the gap equation using the pairing potential (5) we first would like to discuss the reason for its form in more detail. For a continuum system with full translation and rotation symmetry, the pairing potential $V_{\mathbf{kk}'}$ is only a function of $|\mathbf{k}-\mathbf{k}'|$, or the angle between the two wave vectors in view of $|\mathbf{k}|,|\mathbf{k}'|\simeq k_F$ (the Fermi wave vector). Then $V_{\mathbf{kk}'}=V(\hat{\mathbf{k}}\cdot\hat{\mathbf{k}}')$, with $\hat{\mathbf{k}}\cdot\hat{\mathbf{k}}'$ denoting the cosine of the angle between $\mathbf{k}$ and $\mathbf{k}'$, can be expanded in terms of Legendre polynomials. And by use of the spherical harmonic addition theorem, it can be finally written as

$$V(\hat{\mathbf{k}}\cdot\hat{\mathbf{k}}')=\sum_{l=0}^{\infty}V_l\sum_{m=-l}^{l}Y_{lm}(\theta,\phi)Y_{lm}^{*}(\theta',\phi') \tag{6}$$

through spherical harmonics $Y_{lm}(\theta,\phi)$. Obviously the V_s term corresponds to $l=0$ and the V_g term results from the sum of $(l,m)=(4,4)$ and $(4,-4)$. But the cross term $\sim V_{sg}$ in Eq. (5) cannot be obtained from Eq. (6). So we are led to go beyond the above formalism to consider $V_{\mathbf{kk}'}$ as a general function which depends on $\mathbf{k}$ and $\mathbf{k}'$ individually. This will be the case when the fact of having only discrete lattice translation and rotation symmetry is considered. Then the pair potential has to be expanded in terms of the basis functions $\psi_{\Gamma}^{i(l)}(\theta,\phi)$ of the crystal symmetry group (D_{4h}) belonging to a specific irreducible representation Γ of degree l and degeneracy index i. The generalized expansion then reads, suppressing the multiplicity index of Γ,

$$V_{\mathbf{kk}'}=\sum_{\Gamma ll'}V_{\Gamma}^{(ll')}(k,k')\sum_{i}\psi_{\Gamma}^{i(l)}(\theta,\phi)\psi_{\Gamma}^{i(l')}(\theta',\phi')^{*}. \tag{7}$$

For basis functions of different degree l, l' but belonging to the same representation Γ the contribution will generally be nonzero. Then for $\Gamma=A_{1g}$ and $l=0$, $l'=4$ or vice versa one can naturally obtain the nondiagonal contributions $V_{A_{1g}}^{(04)}\propto V_{sg}$ in D_{4h} symmetry.

The pairing potential (5) is therefore a reasonable choice for our problem and we can now solve the corresponding standard BCS gap equation which reads

$$\Delta_{\mathbf{k}}=-\sum_{\mathbf{k}'}V_{\mathbf{kk}'}\frac{\Delta_{\mathbf{k}'}}{2E_{\mathbf{k}'}}\tanh(\beta E_{\mathbf{k}'}/2), \tag{8}$$

where $\beta=1/(k_BT)$ and $E_{\mathbf{k}}=\sqrt{(\varepsilon_{\mathbf{k}}-\mu)^2+\Delta_{\mathbf{k}}^2}$ is the quasiparticle spectrum. $\varepsilon_{\mathbf{k}}$ is the free electron dispersion and μ is the chemical potential. It is easy to check that the gap function (3) is a self-consistent solution of Eq. (8) under the pairing interaction (5), if the gap amplitude Δ and tuning parameter x satisfy the following self-consistent equations:

$$1-x=V_s\sum_{\mathbf{k}}\frac{f(\theta_{\mathbf{k}},\phi_{\mathbf{k}})}{2E_{\mathbf{k}}}\tanh(\beta E_{\mathbf{k}}/2)+V_{sg}\sum_{\mathbf{k}}\psi^{(4)}(\theta_{\mathbf{k}},\phi_{\mathbf{k}})\frac{f(\theta_{\mathbf{k}},\phi_{\mathbf{k}})}{2E_{\mathbf{k}}}\tanh(\beta E_{\mathbf{k}}/2), \tag{9}$$

$$-x=V_g\sum_{\mathbf{k}}\psi^{(4)}(\theta_{\mathbf{k}},\phi_{\mathbf{k}})\frac{f(\theta_{\mathbf{k}},\phi_{\mathbf{k}})}{2E_{\mathbf{k}}}\tanh(\beta E_{\mathbf{k}}/2)+V_{sg}\sum_{\mathbf{k}}\frac{f(\theta_{\mathbf{k}},\phi_{\mathbf{k}})}{2E_{\mathbf{k}}}\tanh(\beta E_{\mathbf{k}}/2). \tag{10}$$

where the angles have been indexed by their corresponding wave vector for clarity. Replacing the summation by integration according to

$$\sum_{\mathbf{k}} \simeq \frac{N(0)}{4\pi}\int_{-\hbar\omega_D}^{\hbar\omega_D} d\xi \int d\Omega,$$

where $\hbar\omega_D$ is an energy cutoff to enforce the constraint $|\varepsilon_{\mathbf{k}}-\mu| \leqslant \hbar\omega_D$ (ω_D: Debye frequency for phonon-mediated SC) and $N(0)$ is the density of states at zero energy for the spectrum $\varepsilon_{\mathbf{k}}-\mu$, we may obtain the following equations:

$$1-x=\frac{1}{4\pi}(\tilde{V}_s I_1+\tilde{V}_{sg} I_2), \tag{11}$$

$$-x=\frac{1}{4\pi}(\tilde{V}_g I_2+\tilde{V}_{sg} I_1). \tag{12}$$

Above, $\tilde{V}_s=N(0)V_s$, $\tilde{V}_g=N(0)V_g$, $\tilde{V}_{sg}=N(0)V_{sg}$ are redefined dimensionless interaction constants, and the integrals $I_{1,2}$ are written as follows:

$$I_1=\int_0^1 d\xi \int d\Omega \frac{f \tanh(\beta\sqrt{\xi^2+\Delta^2 f^2}/2)}{\sqrt{\xi^2+\Delta^2 f^2}}, \tag{13}$$

$$I_2=\int_0^1 d\xi \int d\Omega\, \psi^{(4)} \frac{f \tanh(\beta\sqrt{\xi^2+\Delta^2 f^2}/2)}{\sqrt{\xi^2+\Delta^2 f^2}}, \tag{14}$$

where we use the abbreviated symbols f and $\psi^{(4)}$, and $\hbar\omega_D$ has been taken as the energy unit.

III. NUMERICAL RESULTS

We first consider $V_{sg}=0$, i.e., assume the pairing potential (4). It was found that one or two $s+g$ solutions (i.e., $\Delta>0$, $0<x<1$) may appear when $\tilde{V}_g$ is quite a few times greater than $\tilde{V}_s$. On the other hand, it is easy to check that the pure s wave ($x=0$) and pure g wave ($x=1$) are always trivial solutions. Thus one needs to compare their free energies to find the stable solution. In unit of $N(0)(\hbar\omega_D)^2$ the free energy is given by

$$F=-\frac{1}{2\pi}\int_0^1 d\xi \int d\Omega\left[\sqrt{\xi^2+\Delta^2 f^2}+\frac{2}{\beta}\ln(1+e^{-\beta\sqrt{\xi^2+\Delta^2 f^2}})\right] + \Delta^2(1-x)^2/\tilde{V}_s+\Delta^2 x^2/\tilde{V}_g. \tag{15}$$

Detailed calculation shows that the $s+g$ mixed state is unstable in most of the parameter space. As an example, we have shown in Fig. 2 all the solutions and their relative energies as functions of $\tilde{V}_g$ for fixed $\tilde{V}_s=0.2$ and $T=0$. Two $s+g$ solutions may be present, as shown by the dotted and dashed lines. But compared to the pure s- and/or g-wave solutions, they are found to be energetically unfavorable, see the lowest panel in Fig. 2.[21] Thus the $s+g$ mixture seems very unlikely under the pairing interaction which is the sum of two separable parts (4).

Once $V_{sg}\neq 0$, the above situation changes substantially. Now the pure s and g waves are no longer solutions of Eqs. (11) and (12), i.e., only the possibility of the mixed $s+g$ solutions is present. We have checked within a broad range of V_g/V_s that a single $s+g$ solution exists for nearly all

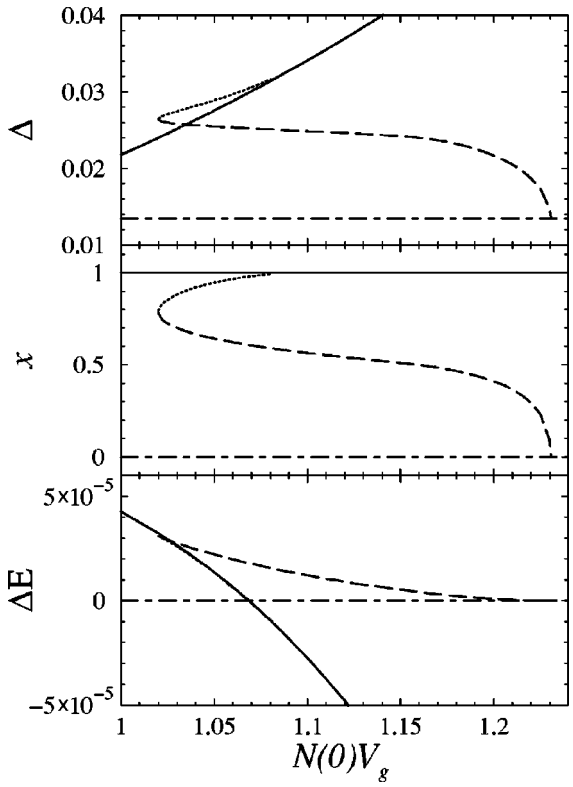

FIG. 2. The parameters Δ, x, and relative energy ΔE as functions of $\tilde{V}_g$ for $\tilde{V}_s=0.2$ ($\tilde{V}_{sg}=0$) and $T=0$. The solid and dot-dashed lines are for pure g- and s-wave solutions, respectively. The dotted and dashed lines are for two possible $s+g$ mixed solutions. The energy of the pure s-wave solution is taken as the reference point in the lowest panel. Energy unit for Δ is $\hbar\omega_D$ and for ΔE is $N(0)(\hbar\omega_D)^2$.

$V_{sg}<0$. As for the realization of the $x=1/2$ $s+g$ state, we discuss the details in the following.

First we consider the special case $V_s=V_g=-V_{sg}$. Then, by adding Eqs. (11) and (12) one can immediately obtain the solution with $x=1/2$ independent of temperature, which means that s and g waves always coexist with equal amplitudes. This result is obvious because in this case the pairing interaction (5) can be simply factorized again into the form $f(\theta,\phi)^* f(\theta',\phi')$ with fixed $x=1/2$. Then only the gap amplitude $\Delta(T)$ is left. It decreases gradually with T and vanishes at the transition temperature T_c, as shown by the dashed line in the upper panel of Fig. 3 where $\tilde{V}_s=0.2$ is used.

Generally, the three interaction parameters have different absolute values. Various situations can be described by tuning these model parameters. We use the following strategy to choose reasonable values: First, we fix the value of $\tilde{V}_s$, e.g., 0.2 throughout the work which sets the overall scale for T_c. Then we assume a value for $\tilde{V}_g$ and tune $\tilde{V}_{sg}$ to realize the $s+g$ state with the constraint $x=1/2$ at $T=0$. Experimentally, the detection of nodes by the field angular-dependent thermal conductivity is applicable only at very low temperatures, i.e., $T \ll T_c$. Thus the measurement actually provides evidence of point nodes only for $T\to 0$, as described by the

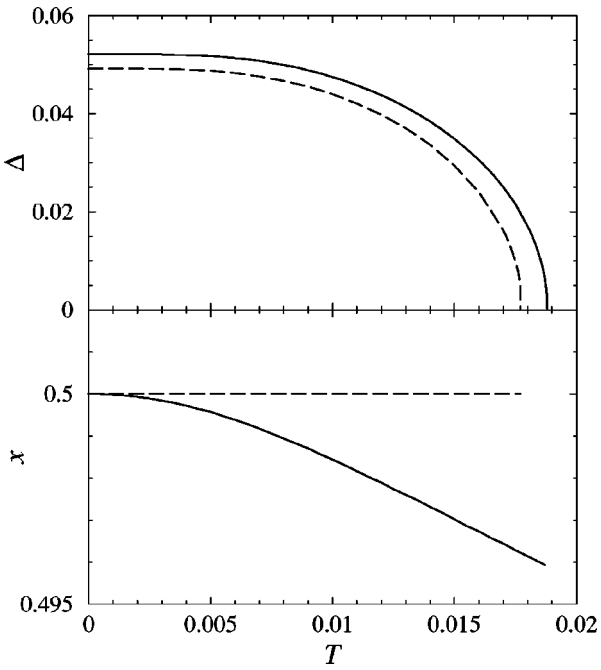

FIG. 3. The order parameter Δ and tuning parameter x as functions of temperature T. Δ and T are in units of $\hbar\omega_D$. The solid lines are for $\tilde{V}_s=0.2$, $\tilde{V}_g=0.1$, $\tilde{V}_{sg}=-0.22$, and the dashed lines are for $\tilde{V}_s=\tilde{V}_g=-\tilde{V}_{sg}=0.2$ corresponding to the special case of T-independent $x=1/2$ $s+g$ wave.

constraint. In this way, the value $\tilde{V}_{sg}$ may be determined for each given $\tilde{V}_g$. We have obtained a nearly linear relation between $\tilde{V}_{sg}$ and $\tilde{V}_g$, as shown in Fig. 4. For example, for $\tilde{V}_s=0.2$ we have $\tilde{V}_{sg}\simeq-0.24+0.2\tilde{V}_g$. With the interaction parameters fixed we can now study an intriguing issue how the $x=1/2$ fine-tuning $s+g$ state at $T=0$ evolves with temperature. One would expect that not only the gap amplitude Δ, but also the tuning parameter x will change with temperature. If it decreases, the node points would cease to exist and a gap would open with increasing temperature. In principle this is indeed observed. As an example, we take $\tilde{V}_g=0.1$. Then $\tilde{V}_{sg}\simeq-0.22$ is obtained to realize the $x=1/2$ $s+g$ solution at $T=0$. Under these interaction parameters $\Delta(T)$ and $x(T)$ are calculated self-consistently from Eqs. (11) and (12). The results are shown by the solid lines in Fig. 3. It is interesting to see that x varies with T monotonically and very slowly. In the current example with $V_g<V_s$, x becomes less than 1/2 at finite T. However, the deviation from 1/2 is less than 1% even at $T=T_c$. This means that a very strong anisotropic gap with $\Delta_{\min}/\Delta_{\max}\leqslant 10^{-2}$ is present in the whole

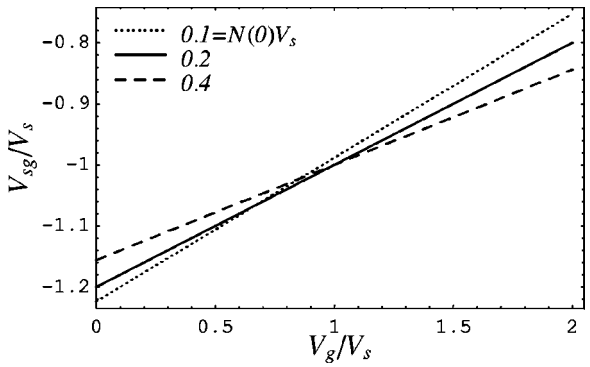

FIG. 4. The required V_{sg}/V_s vs V_g/V_s for a few different $\tilde{V}_s$, in order to realize the $x=1/2$ $s+g$-wave nodal gap function at $T=0$.

superconducting region essentially still describing a gap with point nodes. Thus we conclude that $s+g$ pairing with nodal excitations is a robust solution for all temperatures below T_c and should not be considered as accidental. We also mention that x becomes larger than 1/2 at finite T for the choice of $V_g>V_s$ (not shown), but again only a small deviation is obtained.

IV. CONCLUSION

In the above section, we have obtained a stable hybrid $s+g$-wave state within BCS theory based on the phenomenological pairing interaction (5). Also we have realized the $x=1/2$ hybrid state which has point nodes by an appropriate choice of the interaction parameters. In particular, we have confirmed that the hybrid state with highly anisotropic gap may be robust in the whole superconducting region below T_c. This provides the semiphenomenological theory to understand the $s+g$ ($x=1/2$) gap function proposed by Maki *et al.*[14] Thus the explanation of the experimentally observed point nodes in borocarbides $Y(Lu)Ni_2B_2C$ can be achieved in a self-consistent way. A microscopic theory of our phenomenological pairing model is yet to be developed. Finally we mention that similar $s+g$ mixed gap functions are also proposed very recently for skutterudite $PrOs_4Sb_{12}$,[22] and their justification should be possible based on a similar analysis as presented here.

ACKNOWLEDGMENTS

We thank J. Goryo, K. Maki, and Q. Gu for useful discussions. Q. Yuan acknowledges the support by the National Natural Science Foundation of China (Grant No. 19904007).

[1] P.C. Canfield, P.L. Gammel, and D.J. Bishop, Phys. Today **51** (10), 40 (1998).

[2] *Rare Earth Transition Metal Borocarbides: Superconductivity, Magnetic and Normal State Properties*, edited by K.H. Müller and V. Narozhnyi (Kluwer Academic, Dordrecht, 2001).

[3] S.A. Carter, B. Batlogg, R.J. Cava, J.J. Krajewski, W.F. Peck, and H. Takagi, Phys. Rev. B **50**, 4216 (1994); L.F. Mattheiss, *ibid.* **49**, 13279 (1994); H. Michor, T. Holubar, C. Dusek, and G. Hilscher, *ibid.* **52**, 16165 (1995).

[4] M. Nohara, M. Isshiki, H. Takagi, and R.J. Cava, J. Phys. Soc. Jpn. **66**, 1888 (1997).

[5] M. Nohara, M. Isshiki, F. Sakai, and H. Takagi, J. Phys. Soc. Jpn.

68, 1078 (1999).
[6] K. Izawa, A. Shibata, Yuji Matsuda, Y. Kato, H. Takeya, K. Hirata, C.J. van der Beek, and M. Konczykowski, Phys. Rev. Lett. **86**, 1327 (2001).
[7] T. Park, M.B. Salamon, E.M. Choi, H.J. Kim, and S.I. Lee, Phys. Rev. Lett. **90**, 177001 (2003).
[8] K. Izawa, K. Kamata, Y. Nakajima, Y. Matsuda, T. Watanabe, M. Nohara, H. Takagi, P. Thalmeier, and K. Maki, Phys. Rev. Lett. **89**, 137006 (2002).
[9] E. Boaknin, R.W. Hill, C. Proust, C. Lupien, L. Taillefer, and P.C. Canfield, Phys. Rev. Lett. **87**, 237001 (2001).
[10] I.S. Yang, M.V. Klein, S.L. Cooper, P.C. Canfield, B.K. Cho, and S.I. Lee, Phys. Rev. B **62**, 1291 (2000).
[11] G.-Q. Zheng, Y. Wada, K. Hashimoto, Y. Kitaoka, K. Asayama, H. Takeya, and K. Kadowaki, J. Phys. Chem. Solids **59**, 2169 (1998).
[12] T. Yokoya, T. Kiss, T. Watanabe, S. Shin, M. Nohara, H. Takagi, and T. Oguchi, Phys. Rev. Lett. **85**, 4952 (2000).
[13] P. Martínez-Samper, H. Suderow, S. Vieira, J.P. Brison, N. Luchier, P. Lejay, and P.C. Canfield, Phys. Rev. B **67**, 014526 (2003).
[14] K. Maki, P. Thalmeier, and H. Won, Phys. Rev. B **65**, R140502 (2002).
[15] P. Thalmeier and K. Maki, Acta Phys. Pol. B **34**, 557 (2003).
[16] H. Jang, H. Won, and K. Maki, cond-mat/0302103 (unpublished).
[17] H. Won and K. Maki (unpublished).
[18] S.B. Dugdale, M.A. Alam, I. Wilkinson, R.J. Hughes, I.R. Fisher, P.C. Canfield, T. Jarlborg, and G. Santi, Phys. Rev. Lett. **83**, 4824 (1999).
[19] H.C. Lee and H.Y. Choi, Phys. Rev. B **65**, 174530 (2002).
[20] A. Ghosh and S.K. Adhikari, Physica C **355**, 77 (2001); **370**, 146 (2002))
[21] Only in a narrow region about $1.07<\tilde{V}_g<1.08$, the dotted line, which is indiscernible from the solid one, has the lowest energy, indicating a stable $s+g$ solution with x very close to 1.
[22] K. Maki, H. Won, P. Thalmeier, Q. Yuan, K. Izawa, and Y. Matsuda, cond-mat/0212090, Europhys. Lett. (to be published).